

# Physical limits: Sensitivity, specificity and quantitation:

## Computed Tomography

Fabian Kiessling

Experimental Molecular Imaging  
RWTH-Aachen University, Germany

## $\mu$ CT-Scanners

- $\mu$ CT-scanners vary with respect to design and image processing software
  - Ex vivo bench top systems
    - High resolution imaging (5-50  $\mu$ m)
    - Slow (scan times 10-60 minutes)
    - Usually not gantry based
    - High x-ray dose
  - In vivo  $\mu$ CT-scanners
    - Usually gantry based systems (180° or 360° rotation)
    - Often flat panel detectors
    - Scanners with dual energy function available
    - Moderate resolution (50-150  $\mu$ m)
    - Fast (scan times: 1 sec. - 10 minutes)
    - Lower x-ray dose

## Non Gantry Based $\mu$ CT



Bartling et al., CMIR 2007

- Spatial resolution depend on
- distance between object and detector
  - pixel size at the detector
  - image reconstruction

## „In vivo“ $\mu$ CT scanners



- Spatial resolution depend on
- pixel size at the detector
  - image reconstruction
  - „Real“ spatial resolution should be determined with phantoms (e.g. line pairs in tungsten wire phantoms)

## Quantification

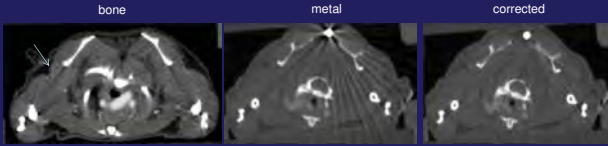
- CT is a quantitative image modality
  - X-ray absorption correlates with measured signal
  - X-ray absorption depend on the photon energy
- **CT number:** quantitative but not calibrated
- **Hounsfield Unit:** CT number normalised for water being 0 and air being -1000
  - Clinically used unit

## Pitfall

- Scanners are often not calibrated
  - CT numbers from different scans are not directly comparable
  - Different values for different energies (voltage)
  - Detector saturation (particularly for flat panels)
    - if object is too small
    - if power (mAs) is too high

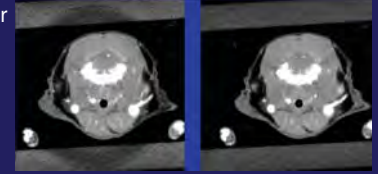
## Artefacts

- Beam hardening artefacts
  - Most detectors do not acquire spectral information
  - Selective removal of soft X-rays from the X-ray beam
  - Linearity not given - loss of information - reconstruction errors
  - If not corrected reduction of the reconstructed attenuation coefficient toward the centre
  - Additional artifacts for bone, metal and CA within the object



## Artefacts

- Ring artefacts
  - Calibration error for single pixels  
(change in pixel sensitivity during and between different scans due to heating)
  - Strong: defect detector pixels /detector line
  - Solution:
    - Interpolation from other pixels
    - Change of detector



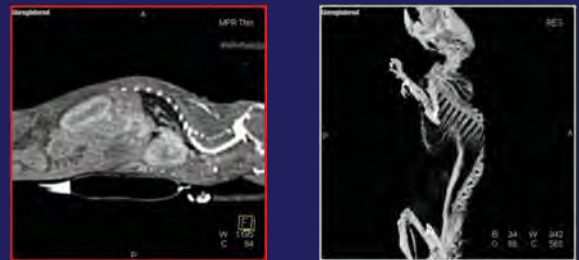
## Potential problems

- Background noise
  - increases with increasing spatial resolution
  - decreases with increasing current
  - 10-30 HU for clinical scanners ((~200µm)<sup>3</sup>)
  - up to 60 HU for µCT-scanners ((50-100µm)<sup>3</sup>)

### Tips:

- Decrease energy (voltage)
- Slow CA injection (careful with postprocessing model)
- Averaging
- Beam hardening correction (not provided by most manufacturers)

## Clinical CA: 4D Perfusion Imaging



- Contrast agent: Imeron 400 (1:1 in NaCl)
- Scan parameters: 80kV, 50mA, 5s rotation time, 4 rotations
- 360° reconstruction 180° overlap

Bartling (DKFZ), Grasruck (Siemens), et al.

## DCE µCT: Data postprocessing

- RBV determination using blood pool CA
- First pass analysis (e.g. Miles model)
- Compartment models
  - Brix
  - Tofts



## Vessel Function: µCT for rBV-Analysis

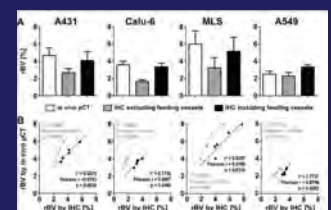
$$rBV (\%) = 100 \times \frac{HU_{\text{tumor}} \text{ after CA} - HU_{\text{tumor}} \text{ before CA}}{HU_{\text{blood}} \text{ after CA} - HU_{\text{blood}} \text{ before CA}}$$

A431: SCC

Calu-6: Lung cancer

MLS: Ovarian cancer

A549: Lung cancer

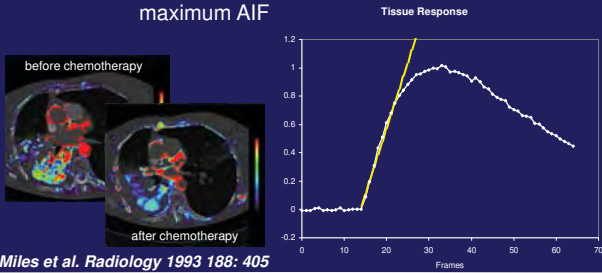


Ehling, Gremse, Lammers et al. (ExMI)

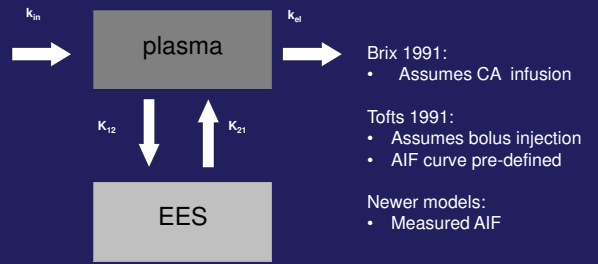
## First pass analysis (Miles model)

Assumption: no CA extravasation during first pass

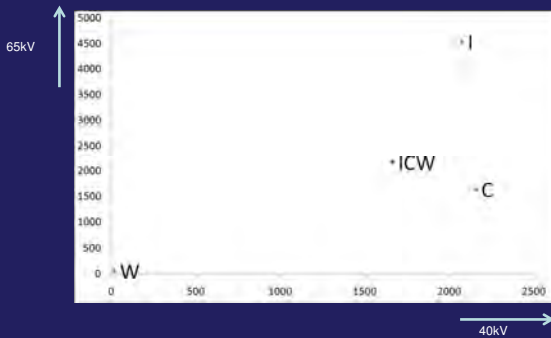
$$\text{Perfusion} = \frac{\text{max. slope tissue fct}}{\text{maximum AIF}}$$



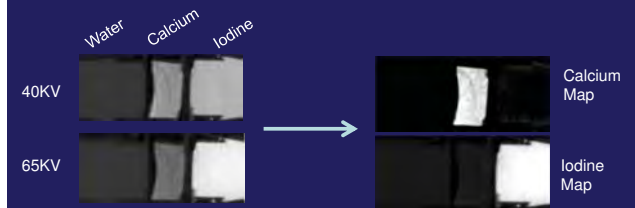
## Two compartment models



## Dual Energy Triangle



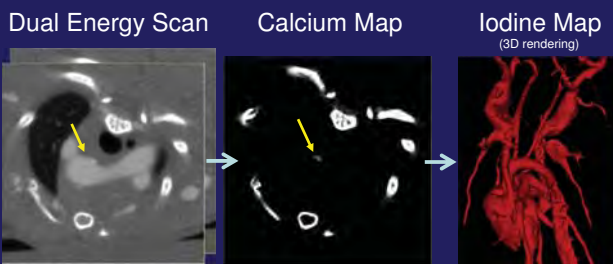
## Dual Energy CT



- Decomposition in three components
- Water, calcium and iodine

Gremse et al., ExMI

## Calcium / Iodine Maps

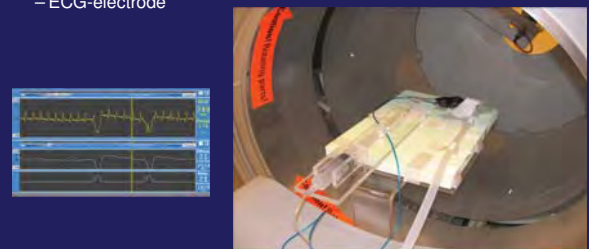


Gremse et al., ExMI

- Atherosclerotic mouse under western diet
- No need for native scan / calcium quantification

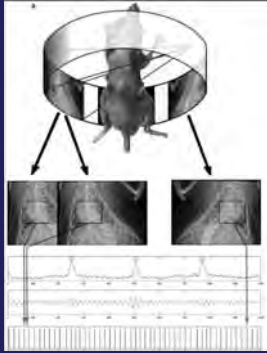
## Cardiac Gating and Breath Triggering

- 1025L Monitoring and Gating System (I4SA); BNC cable (1/0 trigger signal)
  - Pneumatic pillow
  - ECG-electrode



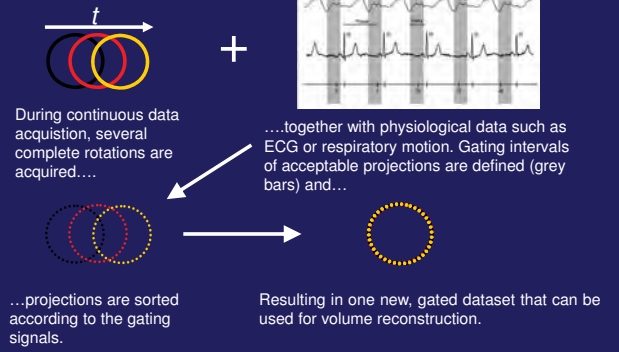
Bartling (DKFZ), Grasruck (Siemens), et al.

## Intrinsic Gating

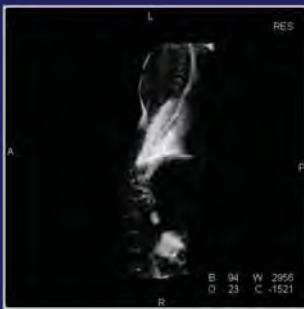


Dinkel, et al. Circulation Cardiovasc. Imaging 2008

## Retrospective Gating

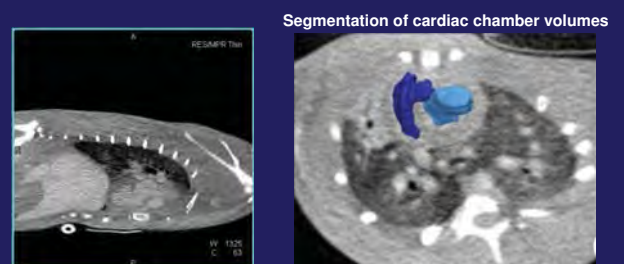


## fpVCT Breath Triggering (Rat)



- Contrast agent: Fenestra (2.5 ml) Bartling (DKFZ), Grasruck (Siemens), et al.
- Scan parameters: 80kV, 50mA, 5s rotation time, 16 rotations

## Blood Pool CA: Cardiac Function



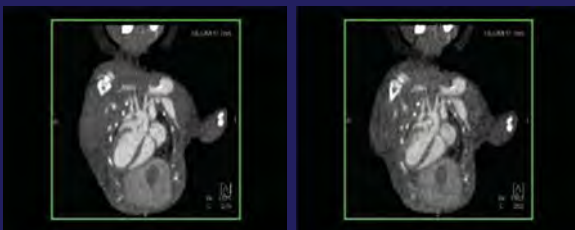
- Scan parameters: 80kV, 50mA, 5s rotation time, 16 rotations
- Breath gating: 20-80% between 2 respirations
- Cardiac gating: 5 equisized phases through cardiac cycle
- Contrast agent: Fenestra (2.5 ml) Bartling (DKFZ), Grasruck (Siemens), et al.

## Cardiac Imaging

### Dobutamin stress test (mouse)

before

after Dobutamin inj.



Dinkel et al., Circulation: Cardiovasc. Imag. (2008)

## Summary

- CT is a versatile quantitative imaging modality
- CT numbers depend on voltage and detector calibration
- Artefacts (beam hardening, rings)
- Background noise
- Perfusion CT
- Dual energy applications
- Motion correction



## **Related Publications “Basic considerations about probes and suitable imaging modalities”**

1. Kalender W., Deak P., Engelke K., Karolczak M. X-Ray and X-Ray-CT. Book title: Kiessling F., Pichler B. Small animal imaging - Basics and practical guide (ISBN 978-3-642-12944-5), Springer, New York: 125-141
2. Bartling SH, Stiller W, Semmler W, Kiessling F. Small animal computed tomography imaging. *Curr Med Imaging Rev* 3, 45-49 (2007).
3. Torchilin VP, Frank-Kamenetsky MD, Wolf GL. CT visualization of blood pool in rats by using long-circulating, iodine-containing micelles. *Acad Radiol* 6(1), 61-65 (1999).
4. Weichert JP, Lee FT Jr, Chosy SG, Longino MA, Kuhlman JE, Heisey DM, Levenson GE. Combined hepatocyte-selective and blood-pool contrast agents for the CT detection of experimental liver tumors in rabbits. *Radiology* 216(3), 865-71 (2000).
5. Bakan DA, Doerr-Stevens JK, Weichert JP, Longino MA, Lee FT Jr, Counsell RE. Imaging efficacy of a hepatocyte-selective polyiodinated triglyceride for contrast-enhanced computed tomography. *Am J Ther* 8(5), 359-65 (2001).
6. Kiessling F, Greschus S, Lichy M, Bock M, Fink C, Vosseler S, Moll J, Mueller MM, Fusenig NE, Traupe H, Semmler W. Volumetric computed tomography (VCT): a new technology for noninvasive, high-resolution monitoring of tumor angiogenesis. *Nat. Med.* 10(10), 1133-1138 (2004).
7. Eisa F, Brauweiler R, Hupfer M, Nowak T, Lotz L, Hoffmann I, Wachter D, Dittrich R, Beckmann MW, Jost G, Pietsch H, Kalender WA. Dynamic contrast-enhanced micro-CT on mice with mammary carcinoma for the assessment of antiangiogenic therapy response. *Eur. Radiol.* 22(4), 900-907 (2012).
8. Gremse F, Grouls C, Palmowski M, de Vries A, Gruell H, Das M, Mühlenbruch G, Akhtar S, Schober A, Kiessling F. Virtual Elastic Sphere Processing Enables Reproducible Quantification of Vessel Stenosis in CT and MR Angiographies. *Radiology*, 260:709-717 (2011).
9. Dinkel J, Bartling SH, Kuntz J, Grasruck M, Kopp-Schneider A, Iwasaki M, Dimmeler S, Gupta R, Semmler W, Kauczor HU, Kiessling F. Intrinsic gating for small-animal CT: A Robust, ECG-less paradigm for deriving cardiac phase Information and Functional Imaging. *Circ. Cardiovasc. Imaging*, 1:235-243 (2008).
10. Mondy WL, Cameron D, Timmermans JP, De Clerck N, Sasov A, Casteleyn C, Piegl LA. Micro-CT of corrosion casts for use in the computer-aided design of microvasculature. *Tissue Eng Part C Methods*, 15:729-38 (2009).